[5] B. Barotcha, W. A. G. Graham, F. G. A. Stone, *J. Inorg. Nucl. Chem.* **1958**, *6*, 119.
[6] J. R. Phillips, F. G. A. Stone, *J. Chem. Soc.* **1962**, 94.
[7] H. C. Brown, N. Ravindran, *J. Org. Chem.* **1977**, *42*, 2733.
[8] D. S. Matteson, R. Soundararajan, *J. Org. Chem.* **1990**, *55*, 2274.
[9] *Organic Syntheses via Boranes*, Wiley-Interscience, New York, NY, **1975**, reprinted edition, *Vol. 1*, Aldrich Chemical Co. Inc., Milwaukee, WI, **1997**, chap. 9.

Ta_4BTe_8: Tantalum Telluride Cluster Chains with Encapsulated Boron Atoms**

Holger Kleinke, E. Wolfgang Finckh, and Wolfgang Tremel*

Clusters of the types $M_6X_{12}^{n+}$ and $M'_8X_8^{m+}$ have been known for many years for Group 5 and 6 transition elements.[1, 2] For the more common M_6X_{12} type, various binary and ternary niobium and tantalum compounds have been made that contain $M_6X_{12}^{2+/3+}$ clusters along with different halide anions.[3, 4] The electronic rules for the stability of these cluster compounds are mainly dictated by the (idealized) cubic symmetry and the connectivity within the cluster cores. The $M_6X_{12}^{n+}$ cluster phases are generally stable for electron counts between 14 and 16;[5] typical electron counts for M_6X_8 clusters range between 19 and 24 with an upper limit of 24.[6] Given the generality that something close to these "magic" electron counts is required for cluster stability, it is clear that the M_6X_8 type is preferred for Group 6 chalcogenides, as observed in the Chevrel phases,[7] whereas the M_6X_{12} type is adopted by Group 5 halides such as Ta_6Cl_{15}.[8]

Analogous clusters of the Group 3 and 4 elements will be seriously electron deficient, but this shortage may be compensated for by encapsulating heteroatoms in the center of the cluster where the heteroatoms donate their electrons to the (otherwise) empty cluster orbitals.[9] Alternatively, to electronically saturate electron-deficient cluster species, counterreduction of the clusters may be achieved by the inclusion of cations into the cluster network.[10] The knowledge of the electronic and structural principles has lead to the discovery of an enormous variety of centered early transition metal halide clusters during the past decade.[11]

So far, a corresponding chalcogenide interstitial cluster chemistry does not exist. McCarley[12] as well as Simon and Köhler[13] developed a systematic chemistry of the "reduced" niobates and molybdates such as $NaMo_4O_6$.[14] The structures of these materials are based on isolated and fused M_6O_{12} units whose inherent electron deficiency is compensated for by charge-balancing cations. In contrast, the structures of early transition metal sulfide, selenide, or telluride clusters are almost exclusively based on Mo_6Q_8 cluster units. Alternative cluster topologies are infinite chains of interpenetrating icosahedral[15] or face-sharing square-antiprismatic units;[16] Ta_2S_2C, which contains layers of edge-sharing C-centered Ta_6 octahedra, is a notable exception.[17]

Here we report on the synthesis, structure, and properties of an unusual centered M_6X_{12} chalcogenide cluster phase. From structural chemistry it is well known that size effects and radius ratios control the structure of materials to a major extent. Similarly, the size of the heteroelement determines the structure of compounds in the sytem M-A-Te (M = Nb, Ta; A = Group 13 element). In attempts to replace gallium (covalent radius $r_{cov} = 1.26$ Å) in the ternary phase $Ta_{13}Ga_3Te_{24}$[18] by the isoelectronic, but much smaller, group homologue boron ($r_{cov} = 0.88$ Å) leads to the formation of the novel cluster compound Ta_4BTe_8 with an interstitial boron atom.[19]

The structure of Ta_4BTe_8 is shown in Figure 1.[20] Ta_4BTe_8 crystallizes in the space group *Pbam* with two formula units per unit cell, and all atoms are situated on mirror planes perpendicular to *c* at $z = 0$ and $\frac{1}{2}$. The structure consists of

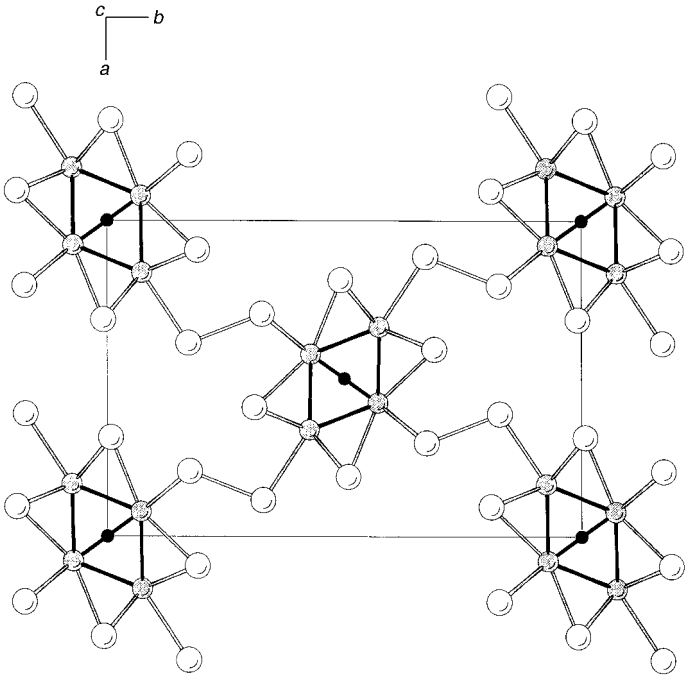

Figure 1. View of the Ta_4BTe_8 structure along *c* (Te: white open spheres, Ta: gray spheres, B: black spheres).

Ta_6BTe_{12} clusters, whose twofold axis is along the viewing direction and which contain a B atom in the center. The individual clusters are condensed by sharing of common edges. As a result, linear chains of centered edge-sharing Ta_6-octahedra are obtained which are coordinated by Te atoms above all free edges and exhibit the connectivity $^1_\infty[Ta1_{4/2}Ta2_2(B)Te1^i_{4/2}Te2^i_{4/2}Te3^a_2Te4^{i-a}_{4/2}]$, according to the nomenclature of Schäfer and von Schnering.[2] Figure 2 shows in

[*] Prof. Dr. W. Tremel, Dr. H. Kleinke, Dr. E. W. Finckh
Institut für Anorganische Chemie und Analytische Chemie der Universität
Duesbergweg, D-55099 Mainz (Germany)
Fax: (+49) 6131-39-3922
E-mail: tremel@indigotrem1.chemie.uni-mainz.de

[**] This work was supported by the Deutsche Forschungsgemeinschaft. We are indebted to Heraeus Quarzschmelze (Dr. Höfer) and the H. C. Starck Co. (Dr. Peters) for material support.

  1433-7851/99/3813-2054 $ 17.50+.50/0

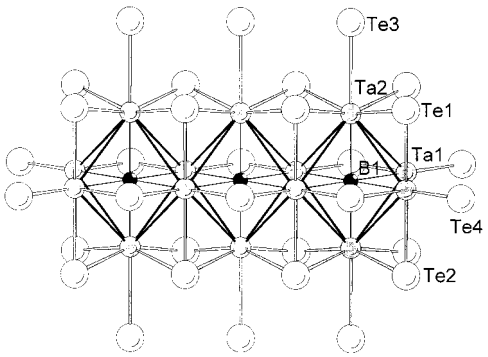

Figure 2. Portion of one infinite cluster chain in the structure of Ta_4BTe_8 with the atomic labeling scheme. Selected distances [Å]: Ta1–B1 2.309(2), Ta2–B1 2.198(3), Ta1–Ta1 2.938(7), Ta1–Ta1 3.564(1), Ta1–Ta2 3.174(4), Ta1–Ta2 3.203(4), Ta2–Ta2 3.564(1), Te1–Ta1 2.803(6), Ta1–Te2 2.735(6), Ta1–Te4 2.848(5), Ta2–Te1 2.783(5), Ta2–Te2 2.752(5), Ta2–Te3 2.939(6), Te3–Te4 2.915(3).

a side view of a portion of one infinite cluster chain of the composition $(Ta_2)(Ta_{4/2})B(Te_2)_{4/2}(Te)_4 \equiv Ta_4BTe_8$. The four crystallographically distinct Te atoms in Figure 2 have three different functions: Four Te1 and Te2 atoms bridge the top and bottom edges of the cluster, two Te4 atoms bridge the equatorial plane, and the Te3 atoms, which are not shared by adjacent clusters of the chain, provide links to parallel but rotated chains ($d_{Te-Te} = 2.786(8)$ Å) according to $Ta_4B(Te^i)_4(Te^{i-a})_2(Te_2^a)$. Thus, the structure is three-dimensional, but highly anisotropic, and the crystals extremely fibrous.

A structural description of Ta_4BTe_8 is based on the hierarchy of interactions. The Ta atoms are surrounded in a pseudooctahedral fashion by Te and B atoms. Ta2, which is situated at the apical position of the Ta_6 octahedra, is surrounded by five Te atoms, and Ta1 at the equatorial plane of the octahedra is surrounded by four Te atoms. The octahedral coordination of Ta2 is completed by one, the coordination environment of Ta1 by two Ta-B contacts ($d_{Ta1-B} = 2.309(2)$ Å $(2\times)$, $d_{Ta2-B} = 2.198(3)$ Å). The equivalence of the two symmetry-independent Te atoms is apparent from the Ta–Te bond lengths, but may also be seen from the computed Ta–Te overlap populations (see below). The average Ta1–Te distance is 2.809 Å and Ta(2)-Te-distance 2.802 Å, in accordance with the structures of related compounds.[21]

The presence of the interstitial boron atom is reflected in the metal–metal distances. Interstitial atoms expand the cluster; thus the average Ta–Ta distance is significantly longer than typical Ta–Ta distances of 2.9–3.0 Å in tantalum halide $[M_6X_{12}]^{n+}$ clusters.[2] The idealized octahedra from which these chains are constructed are characteristically distorted. The Ta–Ta distances at the shared edge ($d_{Ta1-Ta1} = 2.938(7)$ Å) between two adjacent Ta_6 octahedra are comparable to the Ta–Ta distances in Ta metal ($d_{Ta-Ta} = 2.92$ Å). The van der Waals repulsion between the Te atoms along the cluster chains ($d_{Te-Te} = 3.564(3)$ Å) leads to a strong elongation of the Ta_6 octahedra along the chain direction *c*, whereas the average Ta–Ta distance between the apical and equatorial positions of the octahedron is 3.189 Å. Furthermore, the presence of two distinct Ta–B separations may be related to the distortion of the Ta_6 clusters. Ta–B distances correspond to the average M–B distances in B-centered Zr_6 clusters (e.g. $d_{Zr-B} = 2.304$ Å in $K_2Zr_6BCl_{15}$),[22] but they are considerably shorter than typical Ta–B distances in binary borides (e.g. 2.45 Å in Ta_2B).[23] Thus, many structural features of the $[Ta_6BTe_{12}]$ species match those of related clusters among the rare earth halides. Remarkably, chalcogenide cluster compounds containing interstitial atoms are extremely scarce; Ta_2S_2C,[17] $M_{4+x}ATe_4$ (M = Nb, Ta; A = Ga, Si, Cr, Fe, Co), [16] and $Nb_4Te_9OI_4$[24] are the only known examples so far.

Chains of related construction have been found in Sc_4Cl_6Z (Z = B, N)[25] and $NaMo_4O_6$.[14] The principal difference is that in the structure of Sc_4Cl_6Z and $NaMo_4O_6$ the chains are interconnected by isolated chlorine and oxygen atoms, respectively (instead of Te_2^{2-} groups in the case of Ta_4BTe_8), and sodium atoms are located in the cavities between four chains in $NaMo_4O_6$.

It is difficult to describe the electronic structure of Ta_4BTe_8 in simple valence terms. Formal electron counting leads to the formulation $[(Ta^{2.25+})_4(B^{3+})(Te^{2-})_4(Te_2^{2-})_2]$. According to a theoretical analysis for $NaMo_4O_6$, the optimum number of M–M bonding electrons is 13[14b] (compared to 11 for Ta_4BTe_8). Bond order summations using Pauling's formula[26] do not lead to conclusive results. We have performed band-structure calculations using the extended Hückel method[27] to obtain a better understanding of the electronic structure. The density of states (Figure 3) is situated at a small local

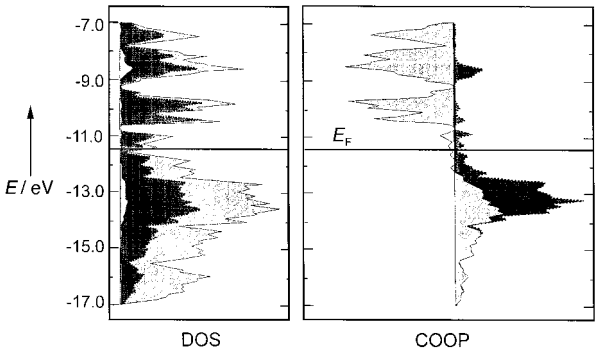

Figure 3. Left: Calculated density of states diagram for Ta_4BTe_8 (light gray: total density, dark gray: Ta contribution, white: B contribution). Right: Obital population analysis of Ta_4BTe_8 (COOP curves; light gray: Ta–Ta, dark dark: Ta–B). The Fermi level is marked by a horizontal bar.

maximum. The projections of the Ta and B contributions in Figure 3 show that the energy states below −15 eV are mainly localized on the Te atoms, whereas the states in the energy window between −15 and −11.5 eV have Ta 5d and Te 5p character with some B 2p admixture. An indication for the highly covalent interactions is the strong mixing of Ta- and Te-centered states in this energy interval. The orbital population analysis[6] (Figure 3) revealed that for Ta_4BTe_8 all strongly Ta–B and Ta–Ta bonding states are occupied, whereas the Ta–Te and Te–Te antibonding states are beginning to be filled. These results are compatible with the picture that, as a consequence of short Te–Te interactions along the chain direction, a fraction of the "anion" states is raised above the Fermi level; therefore, the electron deficiency of Ta_4BTe_8 is less than expected from a comparison with the related oxide

$NaMo_4O_6$. Conductivity studies reveal, in agreement with the computational results, metallic properties for the title compound.

Four-probe single-crystal conductivity measurements along the needle axis *c* show that Ta_4BTe_8 exhibits metallic behavior over the temperature range 4–250 K, with a room-temperature conductivity of 2 $m\Omega^{-1}cm^{-1}$ (Figure 4). No indications of a metal–insulator transition were observed. The electrical conductivity is indicative of a material with a partially filled band at the Fermi level.

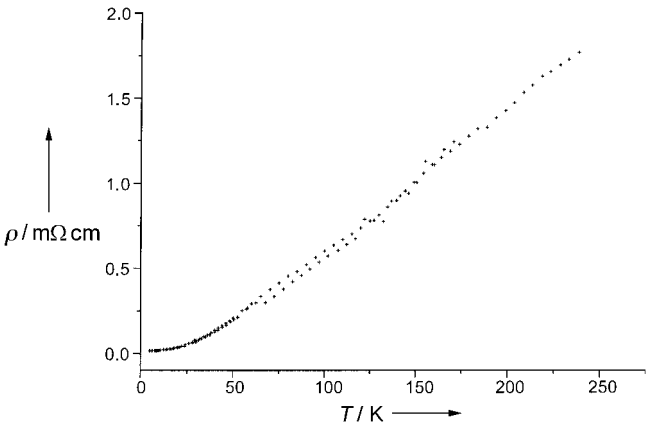

Figure 4. Plot of conductivity versus temperature for a single crystal of Ta_4BTe_8 (measured along the needle axis *c*).

Ta_4BTe_8 provides a conceptual link between the condensed, empty cluster systems encountered among the oxoniobates and oxomolybdates and the condensed rare earth and zirconium halide clusters with interstitial atoms. In the former class of compounds, matrix effects[21] (i.e., the size of the metal oxide clusters) prevents interstitial atoms from being encapsulated in the cluster; the electron deficiency of the cluster is compensated for by countercations in intercluster cavities. On the other hand, the cluster halides of Group 3 and 4 transition metals can "optimize" the cluster electron count by a broad variety of interstitial atoms and additional countercations. Matrix effects do not prevent Group 5 tellurides—formally isoelectronic to the oxoniobates—from balancing their electron deficit by the formation of centered clusters. The smooth encapsulation of boron in Ta_4BTe_8 may be due to thermodynamic (competing boron telluride phases are not stable), structural (cluster proportions optimal for the bonding of boron interstitials), or electronic factors (electron count).

Received: March 6, 1998
Revised version: December 15, 1998 [Z 11561 IE]
German version: *Angew. Chem.* **1999**, *111*, 2189–2192

Keywords: boron · cluster compounds · tantalum · tellurium

[1] A. F. Wells, *Structural Inorganic Chemistry*, 5th ed., Clarendon, Oxford, **1984**, p. 432.
[2] H. Schäfer, H.-G. von Schnering, *Angew. Chem.* **1964**, *20*, 833–849.
[3] F. Rogel, J. Zhang, M. W. Payne, J. D. Corbett, *Adv. Chem. Ser.* **1990**, *226*, 369–389.
[4] A. Simon, *Angew. Chem.* **1981**, *93*, 23–44; *Angew. Chem. Int. Ed. Engl.* **1981**, *20*, 1–22.
[5] F. A. Cotton, T. E. Haas, *Inorg. Chem.* **1964**, *3*, 10–17.
[6] T. Hughbanks, R. Hoffmann, *J. Am. Chem. Soc.* **1983**, *105*, 1150–1162.
[7] R. Chevrel, M. Sergent, J. Prigent, *J. Solid State Chem.* **1971**, *3*, 515–519.
[8] D. Bauer, H.-G. von Schnering, *Z. Anorg. Allg. Chem.* **1968**, *361*, 259–276.
[9] a) A. Simon, *J. Solid State Chem.* **1985**, *57*, 2–23; b) A. Simon, *Angew. Chem.* **1988**, *100*, 164–188; *Angew. Chem. Int. Ed. Engl.* **1988**, *27*, 159–185.
[10] R. P. Ziebarth, J. D. Corbett, *Acc. Chem. Res.* **1989**, *22*, 256–262.
[11] A. Simon in *Clusters and Colloids* (Ed.: G. Schmid), VCH, Weinheim, **1994**, pp. 373–458.
[12] R. E. McCarley, *Polyhedron* **1986**, *5*, 51–61.
[13] J. Köhler, G. Svensson, A. Simon, *Angew. Chem.* **1992**, *104*, 1463–1483; *Angew. Chem. Int. Ed. Engl.* **1992**, *31*, 1437–1456.
[14] a) C. C. Torardi, R. C. McCarley, *J. Am. Chem. Soc.* **1979**, *101*, 3963–3964; b) T. Hughbanks, R. Hoffmann, *J. Am. Chem. Soc.* **1983**, *105*, 3528–3537.
[15] a) H. F. Franzen, J. G. Smeggil, *Acta Crystallogr. Sect. B* **1969**, *25*, 1729–1736; b) H. F. Franzen, J. G. Smeggil, *Acta Crystallogr. Sect. B* **1969**, *25*, 1736–1741; c) B. Harbrecht, *J. Less-Common Met.* **1988**, *138*, 225–234.
[16] M. E. Badding, F. J. Di Salvo, *Inorg. Chem.* **1990**, *29*, 3952–3954; b) K. Ahn, T. Hughbanks, K. D. D. Rathnayaka, D. G. Naugle, *Chem. Mater.* **1994**, *6*, 418–423; b) J. Neuhausen, E. W. Finckh, W. Tremel, *Chem. Ber.* **1994**, *127*, 1621–1624; d) H. Kleinke, E. W. Finckh, W. Tremel, *Eur. J. Inorg. Chem.*, submitted.
[17] O. Beckmann, H. Boller, H. Nowotny, *Monath. Chem.* **1970**, *101*, 945–955.
[18] H. Kleinke, E. W. Finckh, W. Tremel, *Chem. Mater.*, submitted.
[19] Ta_4BTe_8 was synthesized from a mixture (500 mg) of the elements with the molar ratio 1:1:2 in an evacuated quartz tube. I_2 (10 mg) was added as a transport agent. The sample was heated in a furnace at a rate of 1 °C min^{-1} up to 1050 °C and kept at this temperature overnight. Subsequently, the furnace was switched off. After the sample had cooling to room temperature, it was homogenized by grinding and heated in a second quartz tube to 1000 °C. After 10 d the sample was cooled to room temperature radiatively. Long hairlike crystals with a metallic luster had formed. Microprobe analysis of the crystals indicated the presence of tantalum and tellurium in a 1:2 ratio. After the crystal structure of Ta_4BTe_8 had been established, the presence of boron was confirmed by ICP-MS. It was difficult to find crystals of the appropriate size for the X-ray single-crystal structure analysis, as most tended to be very long (>2 mm) and extremely thin (<0.01 mm). After the structure was determined, a powder sample of Ta_4BTe_8 was obtained by heating a stoichiometric mixture of Ta, B, and Te at 1050 °C in an evacuated quartz tube for 10 d. The powder pattern of this material matched the calculated pattern of Ta_4BTe_8.
[20] Data were collected on a Syntex $P2_1$ diffractometer using monochromated $Mo_{K\alpha}$ radiation ($\lambda = 0.71073$ Å) and variable scan speeds of 1.9–19.3° min^{-1}. Crystal size $0.05 \times 0.03 \times 0.18$ mm^3; θ-2θ scan, $2\theta_{max} = 54°$, 1719 reflections, empirical absorption correction (ψ scan), structure solved and refined using the SHELXTL program system, 850 independent reflections, 419 with $F > 6\sigma(F_o)$, $R(F_o)/R_w(F_o) = 0.081/0.067$. The B atom was located as the most prominent peak from a difference Fourier synthesis after the Ta_4B_8 cluster portion of the structure had been refined. Subsequent refinements, where the *U* factor of the B atom was fixed at 0.01 and the occupancy factor was allowed to refine, indicated a full occupancy of the interstitial atom position. Further details on the crystal structure investigation may be obtained from the Fachinformationszentrum Karlsruhe, D-76344 Eggenstein-Leopoldshafen, Germany (fax: (+49) 7247-808-666; e-mail: crysdata@fiz-karlsruhe.de), on quoting the depository number CSD-410843.
[21] T. Saito in *Early Transition Metal Clusters with p-Donor Ligands* (Ed.: M. H. Chisholm), VCH, Weinheim, **1995**, pp. 27–164.
[22] R. P. Ziebarth, J. D. Corbett, *J. Am. Chem. Soc.* **1988**, *110*, 1132–1139.
[23] E. E. Havinga, H. Damsma, P. Hokkelin, *J. Less-Common Met.* **1972**, *27*, 169–175.
[24] W. Tremel, *J. Chem. Soc. Chem. Commun.* **1992**, 709–710.

  1433-7851/99/3813-2056 $ 17.50+.50/0

[25] S. J. Hwu, J. D. Corbett, *J. Solid State Chem.* **1986**, *64*, 331–346.
[26] L. Pauling, *The Nature of the Chemical Bond*, Cornell University Press, Ithaca, New York, **1967**, p. 150.
[27] M.-H. Whangbo, R.Hoffmann, *J. Am. Chem. Soc.* **1978**, *100*, 6093–6098; b) M.-H. Whangbo, R. Hoffmann, R.-B. Woddward, *Proc. R. Soc. London* A **1979**, *366*, 23–46. Ta and Te parameters: W. Tremel, *Angew. Chem.* **1992**, *104*, 230–233; *Angew. Chem. Int. Ed. Engl.* **1992**, *29*, 217–220.

Template-Mediated Synthesis of a Polymeric Receptor Specific to Amino Acid Sequences**

Jens U. Klein, Michael J. Whitcombe, Francis Mulholland, and Evgeny N. Vulfson*

The idea of template-mediated assembly in biological systems was first introduced by Linus Pauling to explain the working of the immune system.[1] We now know this elegant hypothesis to be incorrect but the principle of using a target molecule to create its own recognition site was fruitfully exploited by chemists in the preparation of artificial polymeric receptors by molecular imprinting.[2] The resulting materials have been shown to display specificities similar to polyclonal antibodies[3, 4] and bind ligands with a single dissociation constant.[4, 5] However, it is the recognition of oligonucleotide, -saccharide, or -peptide sequences that is often seen as the real test of the ability of "plastic antibodies" to compete with their natural counterparts. Herein we will address the latter problem by describing the preparation of imprinted polymers specific for amino acid sequences.

Several considerations were taken into account when designing a suitable oligopeptide template[6] for the purpose of this study. Firstly, it was preferable to have a relatively short target molecule such that it could be synthesized in the required quantities by conventional solution-state chemistry. A relatively small target peptide was also preferred as a consequence of the necessity for chemical modification, recovery, and characterization of the template. Secondly, a highly functionalized oligopeptide would enable us to probe the contribution of individual interactions/functional groups by substitutions in the amino acid sequence. At the same time, a net charge of zero would be advantageous to eliminate possible artefacts that arise from nonspecific "ion-exchange type" interactions between the oligopeptide and receptor. Finally, the incorporation of an aromatic amino acid residue in the sequence should facilitate the analysis. Thus, a sequence containing lysine (Lys) and aspartic acid (Asp) in the terminal positions with a bulky tryptophan (Trp) residue in the middle was selected as satisfying all of the above requirements.

The peptide Lys-Trp-Asp (**1**) was preferred to Asp-Trp-Lys for purely synthetic reasons, and the target **1** was prepared in seven steps in 13% overall yield. The synthesis was accomplished by using conventional activated-ester coupling from suitably protected amino acid precursors. A portion of the tripeptide product was then further modified to prepare the template. Carboxylic acids were the natural choice of functionality to interact with amino groups of the lysine residue in the polymer's binding sites. Hence, the tripeptide **1** was treated with 2-methacryloyloxybenzoyl chloride[7] (**2**) to obtain the template **3**. The key feature of this approach is the presence of a relatively labile ester bond between the methacrylic acid residue and the hydroxybenzamide moiety, the cleavage of which would leave the carboxy group in the precise spatial arrangement to interact with the target tripeptide as well as a small "void" in the polymer to facilitate the template removal and re-binding of **1** (Scheme 1).

This simple approach also enabled us to position carboxy groups exclusively in the recognition sites, thus minimizing nonspecific interactions between ligands and the polymeric matrix itself.[8] The carboxylic acid groups of the template **3** were targeted by noncovalent complexation with 2-vinylpyridine[9] (**4**), as depicted in Scheme 1. In order to achieve a reasonable degree of complexation **4** was used in a fourfold molar excess over the template **3**, and the polymerization reaction was carried out in acetonitrile. The choice of solvent was influenced by template solubility and the necessity to stabilize hydrogen-bonding interactions that were essential for the successful imprinting of the tripeptide template. Not only was this important to promote the formation of the complex between the template **3** and monomers **4**, but also to restrict the conformation of the *o*-hydroxybenzamide spacer groups by intramolecular hydrogen bonds. The latter should help to position the methacrylic acid residue precisely in the polymer binding site.[10] Divinylbenzene was selected as the cross-linker to ensure that no degradation of the polymer matrix would occur under the hydrolytic conditions used for template removal. The polymers were prepared photochemically at 4 °C (see the experimental section). Nonimprinted polymer was synthesized under exactly the same conditions, the template being replaced by two equivalents of methacrylic acid, to ensure that the final chemical composition of the polymers were identical.

Once prepared, the polymers were tested with solutions of **1** in aqueous acetonitrile to evaluate their binding properties. Specific binding was seen at all ratios of aqueous/organic solvent (inset in Figure 1) but the binding of **1** to the polymer dropped significantly from 47% in acetonitrile/water 4:1 to 28% in pure water, where the tripeptide was noticeably more soluble. Binding studies were therefore made at 80% acetonitrile where high specific binding and a reasonable range of ligand concentration could be used. Isotherms were then determined for two polymer concentrations (15 and 90 mg mL^{-1}; Figure 1). It is evident from these data that the imprinted polymer shows considerable binding of the peptide, even at concentrations as low as 0.02 mM, while the nonimprinted and the unhydrolysed imprinted polymer (not

[*] Dr. E. N. Vulfson, J. U. Klein, Dr. M. J. Whitcombe, Dr. F. Mulholland
Department of Macromolecular Sciences, IFR, Earley Gate
Whiteknights Road, Reading, RG6 6BZ (UK)
Fax: (+44) 118-926-7917
E-mail: jenya.vulfson@bbsrc.ac.uk

[**] The authors would like to acknowledge the financial support of the BBSRC and the FEBS for granting a fellowship to J.U.K.

  1433-7851/99/3813-2057 $ 17.50+.50/0